

High Efficiency PGM Setup Cycle of Photovoltaic Components via Numerical Simulation

Gabriela Kehlerová¹, Marcel Horák¹, Ivo Matoušek¹

Department of Glass Producing Machines and Robotics, Faculty of Mechanical Engineering, Technical University of Liberec, Liberec, Czech Republic
Email: g.kehlerova@outlook.cz

How to cite this paper: Kehlerová, G., Horák, M. and Matoušek, I. (2025) High Efficiency PGM Setup Cycle of Photovoltaic Components via Numerical Simulation. *Materials Sciences and Applications*, 16, 288-305.

<https://doi.org/10.4236/msa.2025.165017>

Received: April 13, 2025

Accepted: May 26, 2025

Published: May 29, 2025

Copyright © 2025 by author(s) and Scientific Research Publishing Inc. This work is licensed under the Creative Commons Attribution International License (CC BY 4.0).

<http://creativecommons.org/licenses/by/4.0/>



Open Access

Abstract

This study presents a comprehensive analysis of the most important criteria influencing the precision glass molding (PGM) cycle, which was proposed using the finite element (FE) method through the MARC system. The FE models used in numerical simulations were compared with the experimental results of the first phase. The results showed that a significant increase in residual stress in N-BK7 optical glass was manifested in the heating phase in 192 seconds at a temperature of 125°C. The deformation measurement results of selected experimental samples confirmed the high quality of the surface of the moldings and the accuracy of PGM production. Based on the evaluation of the results, the conditions for the production of photovoltaic glass components were proposed.

Keywords

PGM-Precision Glass Molding, Elastic-Plastic and Viscoelastic Behavior, Numerical Simulation, FE-Finite Element

1. Introduction

The development of glass extrusion molding technologies is based on the possibility of utilizing the advantages of direct and indirect molding to produce glass optical elements of complex geometry in a cost-effective manner. Glass, recently redefined as a non-equilibrium, non-crystalline condensed state of matter [1], contains a glass transition region in which it exhibits manifest viscoelastic behavior. Other extremely valuable properties of glass, especially its heat resistance, refractive index, hardness, light transmission, and stability against extreme environmental changes, describe why this material often replaces polymers in many optical applications. Therefore, efficient development and production of optical com-

ponents is a major challenge for the glass industry. Precision glass molding (PGM), as a method of isothermal molding, particularly for small optical parts, can ensure perfect internal and surface quality of the product and high shape accuracy [2]. The production quality of PGM technology is affected by three main problems: shape instability during cooling and after molding, changing optical properties of glass owing to structural relaxation and residual stress, and deterioration of the mold quality. The dependence of the physical and virtual process chains of molding during the development and optimization of glass molding technology is shown in Figure 1.



Figure 1. Development and optimization of glass molding technology - dependence on physical and virtual routes.

An effectively chosen production procedure must simultaneously enable the correction of several factors, preferably using a combination of numerical simulation and verification of the forecast of the result by effective physical modeling. During the molding cycle, glass first passes through the heating phase into a liquid state with a viscosity range of $10^8 - 10^9$ Pa·s at a temperature close to the dilatometric softening point (T_d) in the isothermal PGM process, even above T_d [3]. The glass transition temperature (T_g) is the temperature at which the material changes its behavior from glassy to brittle, elastic, and flexible. The reference viscosity is approximately $10^{11.3}$ Pa·s [4]. The quality of molding, which is significantly affected by residual stress, depends mainly on the temperature history caused by the variability and heterogeneity of the deformations of optical glass [5] [6]. This is an area in the so-called supercooled metastable liquid region, cooling above the glass T_g , which can cause large geometric and qualitative deviations in the glass product. Such complexity often leads to the previously mentioned residual stress and distortion of the molding shape, which causes unexpected defects in the optical function. Molding influenced by residual stress in the formed component changes the refractive index and Abbe number of optical glasses [6]-[9]. For these reasons, the above-mentioned temperature-dependent problems were investigated in this study, and the FE method was used by applying elastic-plastic and viscoelastic models through the MARC system. The Marc system comprises a series of integrated programs that facilitate the analysis of engineering problems in

terms of structural mechanics, heat transfer, and electromagnetics.

2. Methods

2.1. Glass Molding Behavior-Theory

Glass behaves as an elastic solid at low temperatures, and as a Newtonian liquid at extremely high temperatures. For an elastic body, the stress at $t > 0$ is a function of deformation [10]-[13].

$$\sigma(t, \varepsilon_0) = \sigma(\varepsilon_0) = \begin{cases} E(\varepsilon_0) & \varepsilon_0 \text{ nonlinear elastic body,} \\ E & \varepsilon_0 \text{ linear elastic body.} \end{cases} \quad (1)$$

For a viscoelastic body, the stress σ is a function of the deformation ε but also time t :

$$\sigma(t, \varepsilon_0) = \begin{cases} E(\varepsilon_0, t) & \varepsilon_0 \text{ nonlinear elastic body,} \\ E(t) & \varepsilon_0 \text{ linear elastic body.} \end{cases} \quad (2)$$

As previously mentioned, glass behaves viscoelastically near T_g [14]. Unchilled and toughened glass exhibits lower tensile moduli than chilled glass, with the Young's modulus of elasticity E of the clouded glass being lower by approximately 7%. The Poisson's constant μ is the proportionality constant between the relative strain in the stress direction and the relative strain in the direction perpendicular to the applied stress. In the molding temperature range, the stress and strain responses of the glass material strongly depend on time under specific loads. The generalized Maxwell model, which has proven to be an appropriate constitutive model for glass materials, is commonly used to describe such material behavior [15]. In addition to the Maxwell stress relaxation model, the material specification of the FE model can be expanded to include structural relaxation through the Narayanaswamy model (3), which has been used for many years in the FE modeling of technological processes associated with glass production in glass-transition temperature areas. The reference relaxation time τ_{ref} of the glass corresponds to the reference temperature T_{ref} and in general depending on the temperature, the relaxation time can be given as follows:

$$\tau = \tau_{ref} \exp \left[-\frac{\Delta H}{R} \left(\frac{1}{T_{ref}} - \frac{x}{T} - \frac{1-x}{T_f} \right) \right] \quad (3)$$

where x is a fractional parameter with a value of 0 - 1, ΔH is the activation energy, and R is the gas constant. The fractional parameter x determines the extent to which the fictitious temperature affects relaxation time. Typically, for the response function, using assumption (3), the following applies:

$$M_v(\xi) = e^{-\frac{\xi}{\tau}} \quad (4)$$

and for models with n relaxation times:

$$M_v(\xi) = \sum_{i=1}^n (W_g)_i \cdot e^{-\frac{\xi}{\tau_i}} \quad (5)$$

where $(W_g)_i$ is the weighting coefficient, for which it holds that $\sum_i^n (w_g)_i \approx 1$ [16]. Usually, bulk glass deformation behavior at a low strain rate above the yielding point is modeled by the Newtonian incompressible law [17], described in terms of equivalent stress σ and strain rate as given by:

$$\sigma = 3\eta\dot{\epsilon} \quad (6)$$

where η is the viscosity of glass, which can be obtained using the Vogel-Fulcher-Tamman equation. However, Chang *et al.* [18] found that the flow stress function did not follow Newton's exact law for fluids and revised it by modifying the exponent of the strain rate based on their experimental results. A similar phenomenon was observed in this study. According to the properties of the N-BK7 glass, a modified flow equation was adopted in the FE simulation, as follows:

$$\sigma = 3\eta\dot{\epsilon}^{1.2} + 0.3 \quad (7)$$

It should be mentioned that heat transfer continues during pressing. In this case, the heat was transferred to the glass preform from both the upper and lower molds. However, if the glass preform is sufficiently soaked to achieve a uniform temperature distribution within the glass preform during the heating stage, the heat transfer during pressing will be insignificant and will not affect the constants in Equation (7). In order to validate the modified flow Equation (7), it is recommended that rheological experiments be conducted on N-BK7 glass at processing temperatures in the range of 500 - 700 °C, which are typical for precision glass molding applications [19] [20]. Compression or shear tests performed at various strain rates can be used to characterize the stress-strain rate relationship. The resulting experimental data can then be used to empirically determine the material's flow behavior, which may be accurately described using a power-law model of the form:

$$\sigma = K\dot{\epsilon}^n + \sigma_0 \quad (8)$$

In this model, K denotes the strength coefficient, a material constant that characterizes the material's overall resistance to deformation. This parameter is dependent on both temperature and the intrinsic properties of the material. The term $\dot{\epsilon}$ represents the strain rate, which defines the rate at which deformation occurs over time. The exponent n is the strain rate sensitivity, a dimensionless parameter that quantifies the dependence of flow stress on the strain rate. A higher value of n indicates greater sensitivity, meaning that the flow stress increases more significantly with rising strain rate. The parameters K , n , and σ_0 can be determined through nonlinear regression analysis, thereby providing empirical validation and supporting the applicability of the proposed flow model.

The frictional force between the glass and molds during pressing was modeled as constant shear friction [21], which can be defined as:

$$f_s = m\tau_0 \quad (9)$$

where f_s denotes the frictional stress, τ_0 denotes the shear yield stress, and m denotes the friction factor. In this study, a value of 1.0 was assigned to m , assuming

complete adhesion between the glass and molds without slip. Under this condition, the friction stress was a function of the yield stress of the deformed glass. An analysis of the PGM using the FE method was performed with the aim of revealing the mechanism of the course of residual stresses and determining the final shape of the molding. The material specifications used in the MARC system calculations were defined in accordance with theoretical assumptions and available information [22].

2.2. Materials Properties and Boundary Conditions

The Nanotech 140 GPM device on which the experiments for this research were performed was equipped with a single molding chamber with a diameter of 140 mm [23]. In the experiment, the molds were made of HF15 tungsten carbide, the jaws were made of 1.4301 X5CrNi 18-10 stainless steel and the preform was made of N-BK7 optical glass with a cylindrical shape. The detailed thermal and mechanical properties of both the optical glass and the tungsten carbide are listed in **Table 1** [24]-[28]. To prevent oxidation of the molds during heating in the molding chamber, N₂ was used to purge the atmosphere. The aim of this research was

Table 1. Detailed thermal and mechanical properties of optical glass and tungsten carbide.

A. Properties	N-BK7 optical glass	Tungsten carbide forms
Young's modulus of elasticity, E [MPa]	82,500	570,000
Poisson's constant, ν	0.206	0.22
Density, ρ [g/cm ³]	2.51	14.65
Coefficient of thermal expansion, [$^{\circ}\text{C}^{-1}$]	8.3×10^{-6}	-
Thermal conductivity, λ [W m ⁻¹ °C ⁻¹]	1.1	63
Specific heat, C_p [J kg ⁻¹ °C ⁻¹]	858	314
Glass-transition temperature, T_g [°C]	560	-
Fixed coefficient of thermal expansion, α_g [°C ⁻¹]	5.6×10^{-6}	4.9×10^{-6}
Liquid coefficient of thermal expansion, α_l [°C ⁻¹]	1.68×10^{-5}	-
Viscosity, η [M Pa·s] (at 685°C)	60	-
Refractive index n_d , [-]	1.51680 (587.6 nm)	-
B. Structural relaxation parameters used in the numerical simulation		
Reference temperature, T [°C]	685	-
Activation energy/gas constant, $\Delta H/R$ [°C]	47,750	-
Fraction parameter, x^a	0.45	-
Weight factor, w_g	1	-
Structural relaxation time, τ_v [s] (at 685°C)	0.019	-
Stress relaxation time, τ_s [s] (at 685°C)	0.0018	-

A. Thermal and mechanical properties of N-BK7 optical glass and tungsten form carbide;

B. Structural relaxation parameters used in the MARC/Mentat system [24]-[28].

to identify the critical points of the molding cycle, the temperature of the top and bottom of the mold, position of the top mold, the pressing load applied to the molds, and corresponding times recorded in the experiments. The experiments were performed as follows:

a) The molds and the preform were heated to a specified temperature above T_g at a heating rate of 1.05°C/s , and the specified temperature was maintained for a sufficiently long period of time.

b) The preform was molded at a specified temperature and constant speed until the press equipment reached a defined value, after which a constant press load was maintained for the actual molding to take place.

c) Cooling the shaped compact from 610°C to 142°C at an average cooling rate of 0.89°C/s .

After a heating time of 125 s, the preform on the lower mold began to touch the upper mold, and both the load and displacement began to increase from zero, reaching the specified load value at 509 s. Therefore, a constant load of 2500 N was maintained, and the displacement increased over time to an asymptotic value. Furthermore, a creep process occurs in the viscoelastic material, in which the deformation continues to increase at a constant pressure. The remolding of N-BK7 glass occurred in 60 s at $560 - 610^\circ\text{C}$. Four cooling rates were selected to study their effects on the shaped samples. Twenty samples were shaped for five experiments. The aim of the experiment was to verify the molding conditions for the production of a relatively large glass element for photovoltaic panels using the PGM method (**Figure 2**) through the MARC system using the elastic-plastic and viscoelastic models.



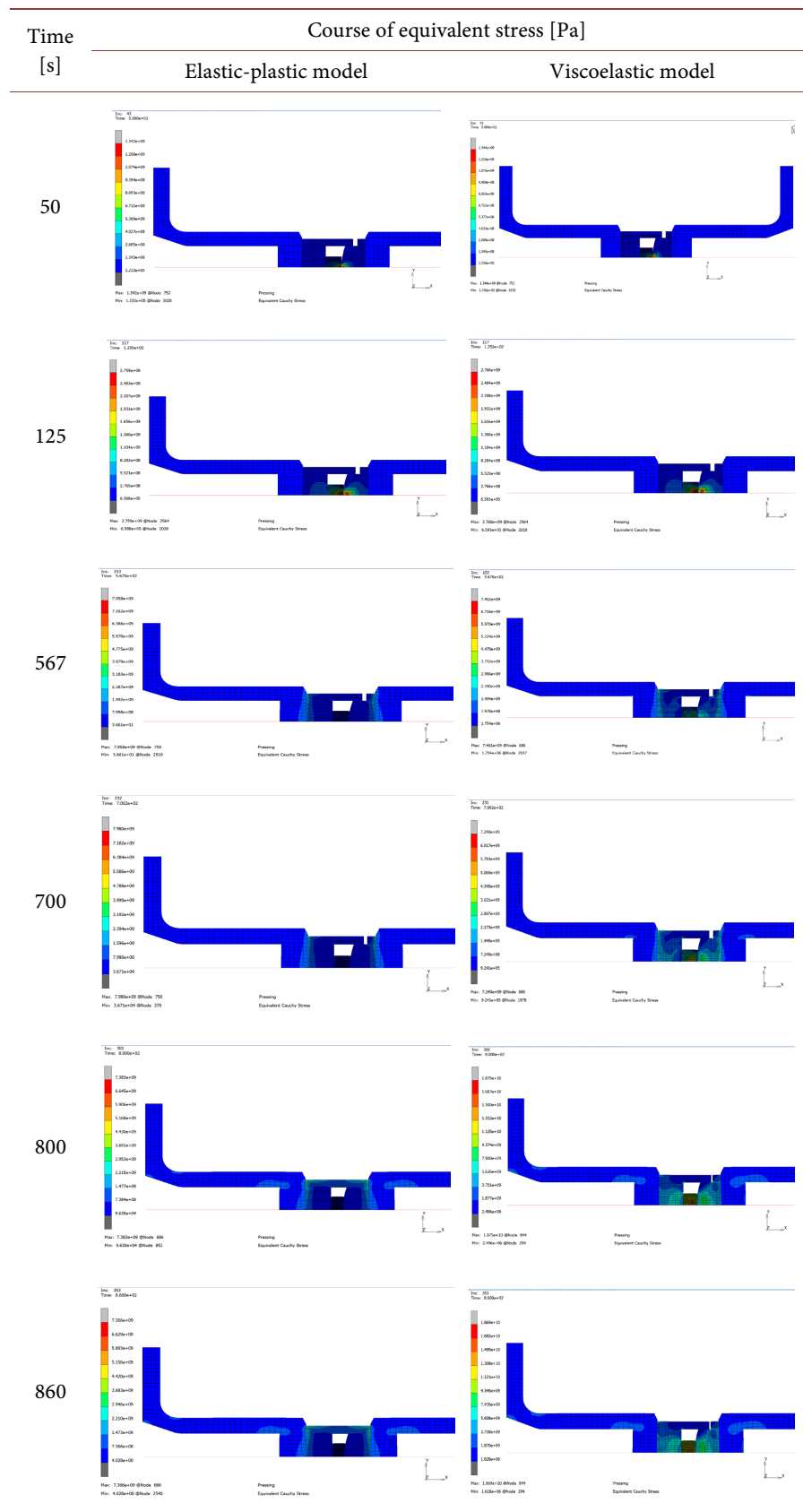
Figure 2. Model of a glass component for producing photovoltaic panels.

3. Results

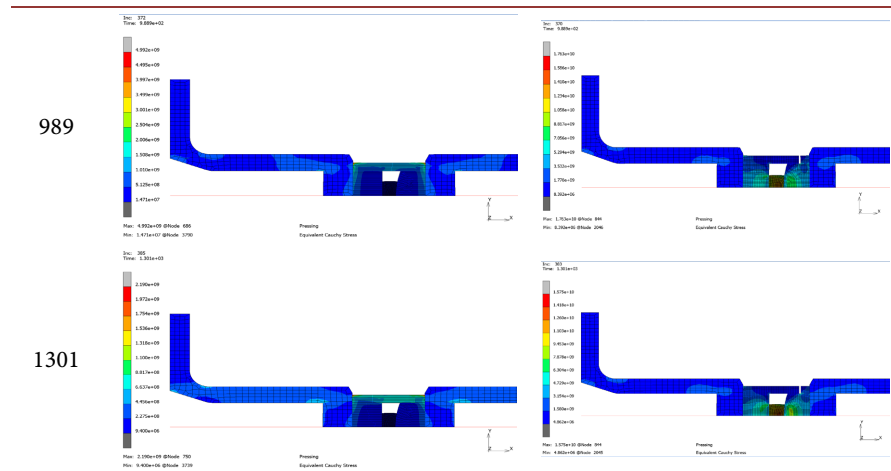
Using dimensional analysis, the key parameters of the molding process were identified by verifying the results. These parameters significantly influenced the production process, resulting shape, and residual stresses of the molding, particularly during the cooling phase. The evaluation of the course of equivalent stress using the elastic-plastic and viscoelastic models in the MARC system as a function of time is presented in **Table 2**.

In both the elastic-plastic and viscoelastic models of the numerical simulation, a significant increase in the stress in the glass was observed during the heating

Table 2. Numerical simulation - course of the equivalent stress as a function of time.



Continued



phase for 192 s at a temperature of 125°C (Figure 3). Subsequent molding of glass occurs under isothermal conditions, either under the action of a constant pressure force or at a constant pressing speed in a defined time interval. At the end of molding process, the glass part is first cooled at a low speed, during which the compressive force remains at an approximately constant level until the temperature of the glass to a value corresponding to the lower cooling temperature ($\eta = 10^{13.5}$ Pa·s). A key parameter of the PGM process that affects the final shape of the product is the residual stress in glass. The residual stress depends mainly on the temperature history in the supercooled metastable liquid region, which is caused by the variability and heterogeneity of optical glass deformations. This is the cooling area above the glass transition temperature, which can cause large geometric and qualitative deviations in the glass product. The results of the numerical simulation for different pressing forces showed a slight relationship between the pressing pressure and residual stress. To study the effect of the pressing temperature on the stress and geometry of the molded lens, the pressing force was set at a constant value of 2500 N, and the temperature was changed from 560 to 610°C.

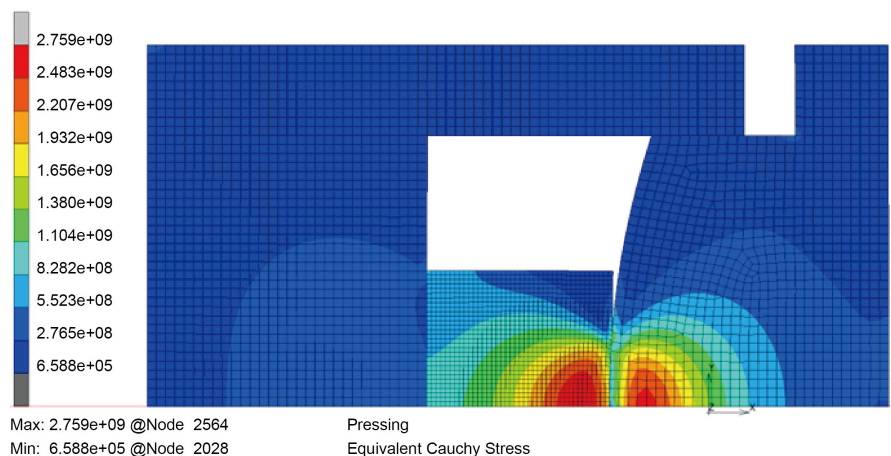


Figure 3. Numerical simulation - equivalent stress at 125°C and time 192 s.

For this reason, the molding process took place under almost isothermal conditions in the optimal region above the glass-transition temperature, in which the material had an unstable non-equilibrium structure, and the viscosity of the glass ranged from 10^8 to 10^{12} Pa·s. The resulting shape of the curve, showing the course of the equivalent stress of the upper part of the mold and the N-BK7 glass as a function of time, was not the same in the numerical simulation for the elastic-plastic model and viscoelastic models (**Figure 4**). Using the viscoelastic model, the increasing internal stress manifests slightly earlier in the glass than in the mold, particularly during the rapid cooling phase. Excessive stress on the edge of the glass element caused by an incorrect cooling rate can easily cause the molding to crack in practice. By applying the elastic-plastic model, the course of the equivalent stress in the glass and upper part of the mold was most pronounced in the molding phase. The stress in the glass increased rapidly during the heating phase, until it approached the glass transition temperature. It is evident that the maximum stress appeared particularly at the edge and center of the glass element. Although the effect of pressure was insignificant, it was not observed during the molding phase when an equivalent stress was applied. The value of the pressed glass elements increased with time. With increasing temperature, the maximum

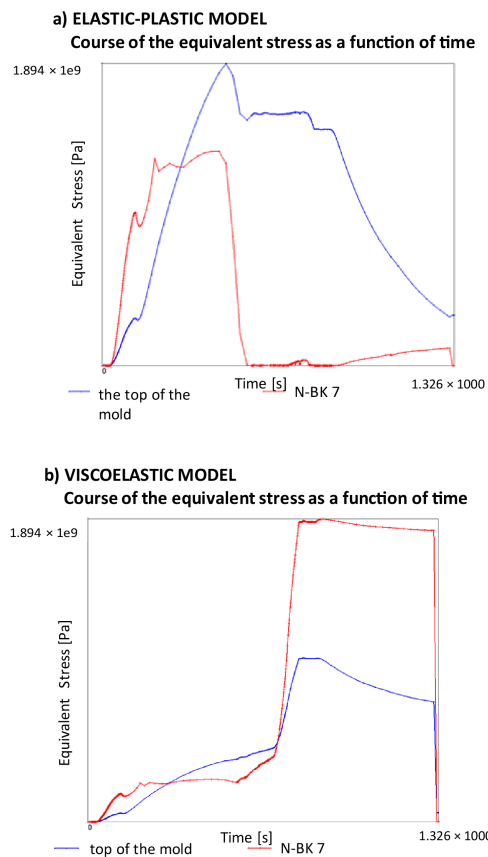


Figure 4. Course of the equivalent stress of the upper part of the mold and N-BK7 glass as a function of time a) elastic-plastic model, b) viscoelastic model.

residual stress of the element decreased, leading to better flowability and lower glass viscosity. Furthermore, owing to structural relaxation in this temperature interval, the atomic structure that controls the properties of the material is strongly dependent on the time and temperature history. This makes the PGM process extremely sensitive to the molding temperature. This complexity often leads to residual stress and shape distortion in the molded lens, causing unexpected defects in its optical function. Evaluation of the numerical simulation results clearly confirmed that the internal stress of the N-BK7 glass was very small during the pressing phase. Based on the dependence of the equivalent stress on the molding temperature, it is possible to create an approximation of the molding conditions for the prediction of production parameters during the development of a photovoltaic component. It is also necessary to consider that the residual stress of the glass parts leads to a refractive index that negatively affects the quality requirements of the optical properties of the molding (the refractive index of N-BK7 is 1.517 at 587.6 nm) [29] [30]. A combination of both models was used to capture the complex behavior of glass that exhibited both time-dependent and permanent deformation. The viscoelastic model is preferred for glass where time-dependent behavior (creep and stress relaxation) is important and useful for capturing the behavior of materials under cyclic loading. Verification of the FE outputs with the experimental results in the laboratory showed excellent agreement with the results, which confirmed the validity of our method for the further development of photovoltaic glass components.

4. Discussion

The production parameters, which were compared to the values of the pressed glass parts for each numerical simulation, show how the volume and profile of the glass part change depending on the change in the process parameters. To evaluate the quality and shape of optical components, RMS methods (e.g., Root Mean Square (RMS) and PV (peak) methods) are most often used in production practice. Although the PV and RMS values were calculated from the same data as the interferometer measurements, their meanings were quite different.

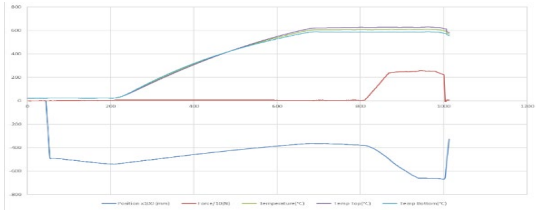
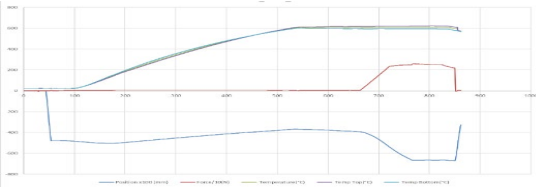
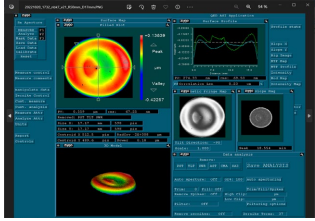
Surface Evaluation

The results of the PV/W measurements of the moldings selected from the PGM production process are presented in **Table 3**. The calculated values of the radius of curvature of the upper part of the N-BK7_R 50 mm and N-BK7_R 100 mm moldings are almost comparable. The radius of curvature of the upper part of the N-BK7_R 200 mm molding was 0.47% higher than that of the N-BK7_R 100 mm molding, which was significantly reflected in the higher deformation of the surface of the glass molding. The edges between the surfaces are visibly rounded in the N-BK7_R 200 mm molding, particularly in samples 19 and 20. The typical PV/W values of machine-ground and polished glass components have a maximum value of 0.7 and a maximum radius of curvature <100 μm . The surface deformation of experimental samples in **Table 3** confirms the need to know the criteria of the

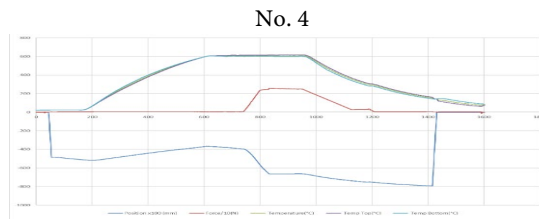
isothermal molding process for determining the most suitable initial and boundary conditions of the PGM process. The evaluation of the deformation measurement results of all the experimental samples confirmed the high quality and accuracy of the PGM. In manufacturing practice, it is quite common for the radius of curvature to be less than 100 μm . The surface deformation of selected experimental samples in **Table 3** confirms the necessity of determining the manufacturability criteria based mainly on the PV value. For most optical products, an ideal value of 1/10 PV is required without specifying the test conditions and with a minimal budget. This results in an unmanufacturable component, an overestimated price, or a reinterpreted specification by the supplier. During the production process, it is nearly impossible to obtain an absolute 1/10 PV. Considering the possibility of a close analogy with the occurrence of errors in a PGM system, the performance impact of each parameter may only relate to the ability to match a particular error in the final system.

Table 3. Deformation of the surfaces and the radius of curvature of the edges of experimental samples a) the upper part of the N-BK7_R 50 mm molding, b) the upper part of the N-BK7_R 100 mm molding and c) the upper part of the N-BK7_R 200 mm molding.

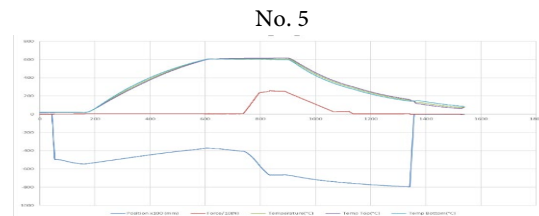
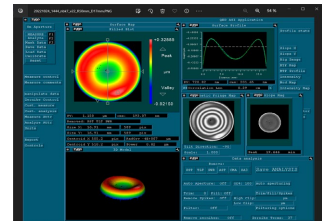
a) The upper part of the N-BK7_R 50 mm molding.				
Sample No.	Size of one pixel [mm]	Number of pixels [pix]	PV [μm]	PV/W
01	17.570	612	0.795	0.07
03	17.170	598	0.559	0.05
05	16.910	589	1.150	0.12
07	17.000	592	1.264	0.13
Average:				0.09

Experiment No. N-BK7 molding cycle process	Sample No. Surface Deformation
No. 1	Sample 01_R50 mm D17 mm
	
No. 3	Sample 03_R50 mm D17 mm
	

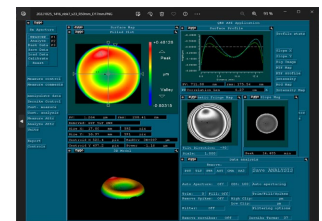
Continued



Sample 05_R50 mm D17 mm



Sample 07_R50 mm D17 mm

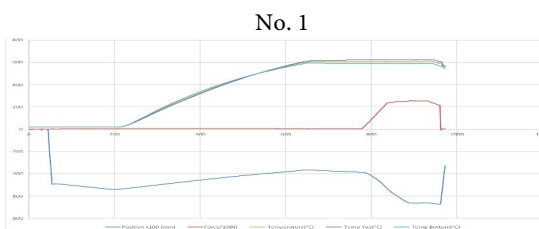


b) The upper part of the N-BK7_R 100 mm molding.

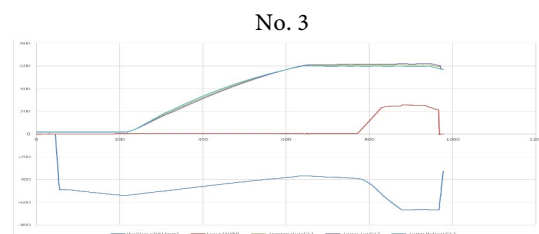
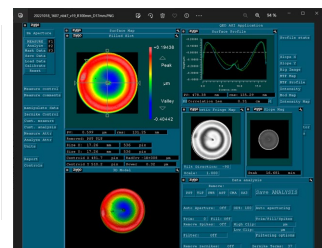
Sample No.	Size of one pixel [mm]	Number of pixels [pix]	PV [μm]	PV/W
08	17.26	536	0.599	0.06
10	16.97	527	0.516	0.06
12	16.94	526	1.057	0.12
Average:				0.08

Experiment No.
N-BK7 molding cycle process

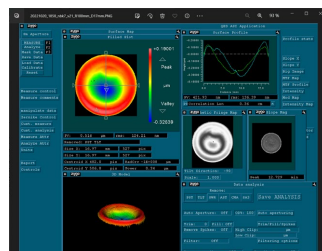
Sample No.
Surface Deformation



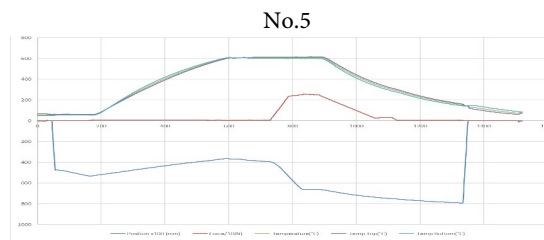
Sample 08_R100 mm D17 mm



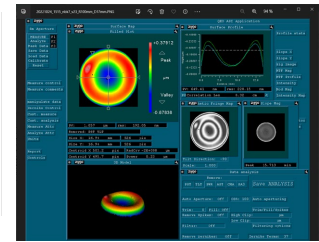
Sample 10_R100 mm D17 mm



Continued



Sample 12_R100 mm D17 mm



c) The upper part of the N-BK7_R 200 mm molding.

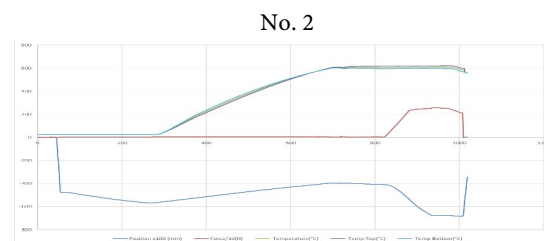
Sample No.	Size of one pixel [mm]	Number of pixels [pix]	PV [μm]	PV/W
16	17.11	310	0.521	0.10
17	17.17	311	0.334	0.06
20	16.89	306	1.213	0.23
19	16.89	306	1.056	0.20

Average:

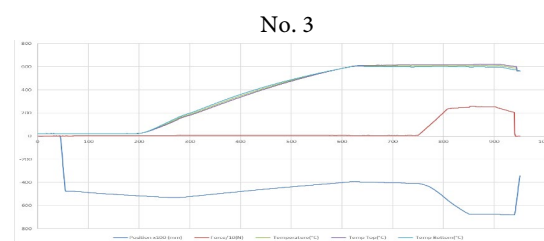
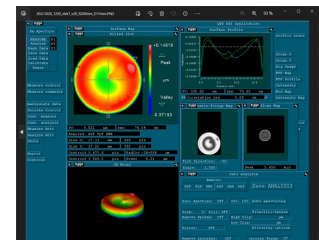
0.15

Experiment No.
N-BK7 molding cycle process

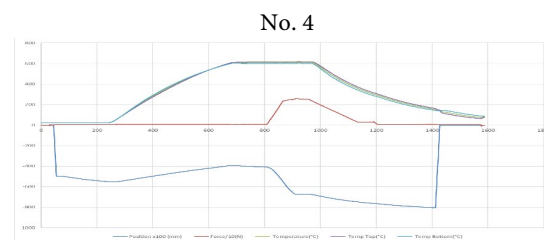
Sample No.
Surface Deformation



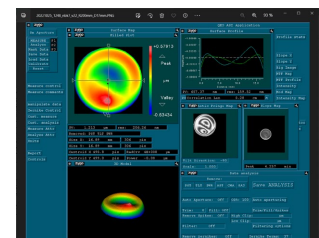
Sample 16_R200 mm D17 mm



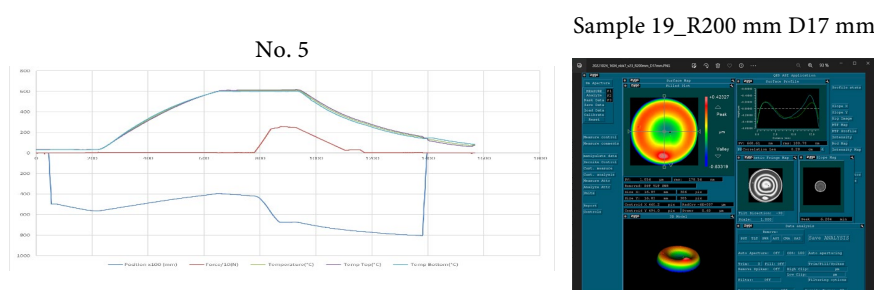
Sample 17_R200 mm D17 mm



Sample 20_R200 mm D17 mm



Continued



By evaluating the measured data, it is possible to conclude that:

a) The change in conditions during the rapid cooling phase in experiments No. 4 and No. 5 had a significant impact on the reduced quality of the surface of the molding compared with the course of experiment No. 1-3.

b) The different rounding radii of the upper parts of the mold have an almost negligible effect on the quality of the molded surface.

Based on the MARC results, it was confirmed that the internal stress of the N-BK7 glass was negligible during the pressing phase.

Based on the MARC results, it was confirmed that the internal stress of the N-BK7 glass was negligible during the pressing phase.

Because the maximum stress increases with an increase in molding speed, it is possible to assume that the degree of cooling in the PGM process above the glass transition temperature of N-BK7 can cause large deformations in the glass molding. At the same time, it is necessary to take into account that the residual stress of the glass leads to a change in the refractive index, which significantly affects the requirements for the quality of the optical properties of the molding. This initial FE model must be further developed and refined in accordance with physical testing for further successful verification and use of the obtained data in the preproduction phase. The results of measuring the deformation of selected experimental samples confirmed the high quality of the surface of the moldings and the accuracy of the PGM production. The study showed that the degree of cooling in the PGM process above the glass transition temperature of N-BK7 can cause large deformations in the shape of glass molding. Because the maximum stress increases with the increase in the molding speed, it is possible to assume that the entire molding cycle at this speed of 0.1 mm/s will be more suitable, especially for molding a glass part with a large diameter, i.e., also for a glass component for photovoltaic components.

Compensation of Lens Profile Deviation in PGM via FE Method

This study demonstrated that residual stress development in the PGM process is strongly influenced by temperature history, especially in the supercooled liquid region above the glass transition temperature. Numerical simulations using both elasticplastic and viscoelastic models revealed distinct stress patterns, with the viscoelastic model better capturing time-dependent behaviors such as creep and

stress relaxation. Higher molding temperatures resulted in lower residual stress due to improved flowability and reduced viscosity. Residual stresses, particularly at the edges and center of the glass element, can lead to geometric distortion and changes in refractive index affecting the optical quality of components like N-BK7 glass. Accurate prediction and control of these stresses are essential for meeting optical performance standards. Key influencing factors include annealing rate, temperature distribution, hold-up force, release temperature, and interfacial heat transfer. Obviously, velocity vector distribution in the outer region of the glass piece is very uniform. From this point, we can say that choosing a suitable heating time is not only an important issue for prolonging the service life of molds, but also an essential step for improving form accuracy and optical property of the molded lenses. The initial maximum profile deviation of approximately 9 μm exceeds the accuracy requirements of high-precision optical lenses, which typically demand tolerances within $\lambda/4$ (0.1 - 0.2 μm). To address this, mold compensation was employed by incorporating the simulated deviation profile into the mold geometry. This iterative process, though traditionally time-consuming and costly, can be efficiently guided using FE simulations. In this study, after compensation, the maximum deviation was reduced to approximately 0.04 μm , well within the acceptable range. These results confirm that FE simulation based mold compensation is an effective method for improving the accuracy and performance of precision-molded glass lenses. The strong agreement between simulation and experimental results validates the modeling approach and highlights the need for further investigation into the coupling between processing parameters, residual stress, and optical properties in advanced glass components.

5. Conclusions

This study presents a comprehensive analysis of the most important criteria influencing the PGM cycle, which was proposed using numerical simulation. The outputs of the FE models used in the numerical simulations were compared to the experimental results of the first phase. Their mutual comparison confirmed a significant agreement between the simulation and real course of the PGM molding cycle. In the next phase, the evaluation of the experiments performed verified the fundamental effects on the resulting quality of molding with different shapes. The setting of the Nanotech 140 GPM device was evaluated as the most suitable for experiment No. 3, where the lowest rate was applied in the gradual slow cooling phase, i.e., at 1/4 of the initial value used in experiments No. 1, 4, and 5. This setting resulted in a significantly higher-quality molded surface. Surface irregularities or deformations were analyzed to assess the quality of the molding, and the quality of processing was evaluated according to the sampling plan. Based on the evaluation of the results, the conditions for the production of photovoltaic glass components were proposed.

While the findings provide valuable insights, the study is limited by its focus on a single geometric configuration. In real-world applications, precision glass com-

ponents often possess aspherical or freeform geometries, which introduce more complex thermal and mechanical boundary conditions, potentially leading to different residual stress distributions and deformation behaviors. To enhance the generalizability and practical relevance of this work, future research should incorporate a wider range of geometrical profiles.

Acknowledgements

The results were obtained with support from the Department of Glass Machinery and Robotics of the Faculty of Mechanical Engineering at the Technical University of Liberec. The authors thank the department management for supporting the research activities in the field of glass and numerical simulations.

Author Contributions Statement

All the above-mentioned authors contributed equally to the manuscript.

Ethics Statement

The authors declare that there are no ethical issues associated with this article.

Data Access Statement

All relevant data are presented in the paper and its Supporting Information files.

Funding Statement

This study was conducted under the research program SGS-2023-5393 of the Technical University of Liberec. The funders had no role in the study design, data collection and analysis, decision to publish, or manuscript preparation.

Conflicts of Interest

The authors declare no conflicts of interest regarding the publication of this paper.

References

- [1] Zanotto, E.D. and Mauro, J.C. (2017) The Glassy State of Matter: Its Definition and Ultimate Fate. *Journal of Non-Crystalline Solids*, **471**, 490-495.
<https://doi.org/10.1016/j.jnoncrysol.2017.05.019>
- [2] Chang, C.J., Chao, C.L., Chou, W.C., Chen, Y.K., Ma, K.J. and Chen, C.C. (2012) Simulation and Experimental Analysis of Moulding Processes of Glass Diffractive Optical Elements. *Applied Mechanics and Materials*, **217**, 1646-1649.
<https://doi.org/10.4028/www.scientific.net/amm.217-219.1646>
- [3] Vallet, G. (2011) Stress Relaxation of Glass Using a Parallel Plate Viscometer, Materials Science, Physics. The Graduate School of Clemson University.
- [4] Holly, C., Traub, M., Hoffmann, D., Widmann, C., Brink, D., Nebel, C., *et al.* (2016) Monocrystalline CVD-Diamond Optics for High-Power Laser Applications. *SPIE Proceedings*, San Francisco, 18 March 2016, Article 974104.
<https://doi.org/10.1117/12.2213601>
- [5] John Deegan Rochester Precision Optics (2007) Precision Glass Molding Technical

Brief, Rochester Precision Optics.

- [6] Schaub, M., Schwiegerling, J., Fest, E.C., *et al.* (2016) *Molded Optics: Design and Manufacture*. Optical Sciences, Ophthalmology and Vision Sciences. CRC Press.
- [7] Su, L., Wang, F., He, P., Dambon, O., Klocke, F. and Yi, A.Y. (2014) An Integrated Solution for Mold Shape Modification in Precision Glass Molding to Compensate Refractive Index Change and Geometric Deviation. *Optics and Lasers in Engineering*, **53**, 98-103. <https://doi.org/10.1016/j.optlaseng.2013.08.016>
- [8] Zhao, W., Chen, Y., Shen, L. and Yi, A.Y. (2009) Refractive Index and Dispersion Variation in Precision Optical Glass Molding by Computed Tomography. *Applied Optics*, **48**, 3588-3594. <https://doi.org/10.1364/ao.48.003588>
- [9] Sojecki, A. (1995) Changes of the Refractive Index during the Molding Process. *SPIE Proceedings*, San Diego, 8 September 1995, 475-477. <https://doi.org/10.1117/12.218454>
- [10] Vallet, G.M. (2011) *Stress Relaxation of Glass Using a Parallel Plate Viscometer*. Clemson University.
- [11] Findley, W.N., Lai, J.S., *et al.* (1989) *Creep and Relaxation of Nonlinear Viscoelastic Materials*. Dover Publications.
- [12] Findley, W., James, N., Lai, S., *et al.* (1976) *Creep and Relaxation of Nonlinear Viscoelastic Materials with an Introduction to Linear Viscoelasticity*. North Holland.
- [13] Hult, J.A.H. (1966) *Creep in Engineering Structures*. Blaisdell.
- [14] Varshneya, A.K. and Mauro, J.C. (2019) *Fundamentals of inorganic Glasses*. Elsevier. <https://doi.org/10.1016/C2017-0-04281-7>
- [15] Gy, R., Duffrène, L. and Labrot, M. (1994) New Insights into the Viscoelasticity of Glass. *Journal of Non-Crystalline Solids*, **175**, 103-117. [https://doi.org/10.1016/0022-3093\(94\)90002-7](https://doi.org/10.1016/0022-3093(94)90002-7)
- [16] Schwarzl, F. and Staverman, A.J. (1952) Time-Temperature Dependence of Linear Viscoelastic Behavior. *Journal of Applied Physics*, **23**, 838-843. <https://doi.org/10.1063/1.1702316>
- [17] Rouxel, T., Huger, M. and Besson, J.L. (1992) Rheological Properties of Y-Si-Al-O-N Glasses—Elastic Moduli, Viscosity and Creep. *Journal of Materials Science*, **27**, 279-284. <https://doi.org/10.1007/bf02403674>
- [18] Chang, S.H., Lee, Y.M., Jung, T.S., Kang, J.J., Hong, S.K., Shin, G.H., *et al.* (2007) Simulation of an Aspheric Glass Lens Forming Behavior in Progressive GMP Process. *AIP Conference Proceedings*, **908**, 1055-1060. <https://doi.org/10.1063/1.2740950>
- [19] Ito, H., Arai, M., Kodera, T. and Ino, T. (2010) Strain Rate and Temperature Dependences on Strength Property of Glass Material. *Journal of Solid Mechanics and Materials Engineering*, **4**, 1511-1519. <https://doi.org/10.1299/jmmp.4.1511>
- [20] Sarhadi, A., Hattel, J.H. and Hansen, H.N. (2014) Precision Glass Molding: Validation of a Fe Model for Thermo-Mechanical Simulation. *International Journal of Applied Glass Science*, **5**, 297-312. <https://doi.org/10.1111/ijag.12071>
- [21] Li, G., Jinn, J.T., Wu, W.T. and Oh, S.I. (2001) Recent Development and Applications of Three-Dimensional Finite Element Modeling in Bulk Forming Processes. *Journal of Materials Processing Technology*, **113**, 40-45. [https://doi.org/10.1016/s0924-0136\(01\)00590-8](https://doi.org/10.1016/s0924-0136(01)00590-8)
- [22] Fujidie (2003) *Material: Cemented Carbide Alloys*. <https://www.fujidie.co.jp/path-to-document.pdf>
- [23] <https://opg.optica.org/ao/abstract.cfm?uri=ao-54-22-6841>

- [24] Jain, A. (1963) Experimental Study and Numerical Analysis of Compression Molding Process for Manufacturing Precision Aspherical Glass Lenses. Ph.D., Thesis, The Ohio State University.
- [25] Schott, A.G. (n.d.) N-BK7|Optical Borosilicate-Crown Glass from SCHOTT|BK 7 (Pgo-Online.com). <https://www.schott-datasheet-n-bk7-eng.pdf>
- [26] Jain, A. (2006) Experimental Study and Numerical Analysis of Compression Molding Process for Manufacturing Precision Aspherical Glass Lenses. Dissertation, The Ohio State University.
- [27] <https://www.paganoni.it/en/articles-blog/tungsten-carbide-characteristics-applications-and-properties>
- [28] Plastic Technology Ltd. (1992) Sandvik H15F Extra-Fine Grain Cemented Carbide for Rotary Tools.
- [29] Chen, Y., Yi, A.Y., Su, L., Klocke, F. and Pongs, G. (2008) Numerical Simulation and Experimental Study of Residual Stresses in Compression Molding of Precision Glass Optical Components. *Journal of Manufacturing Science and Engineering*, **130**, Article 051012. <https://doi.org/10.1115/1.2950062>
- [30] Liu, W. and Zhang, L. (2015) Thermoforming Mechanism of Precision Glass Moulding. *Applied Optics*, **54**, 6841-6849. <https://doi.org/10.1364/ao.54.006841>